

# Subwavelength confinement in an integrated metal slot waveguide on silicon

Long Chen, Jagat Shakya, and Michal Lipson

*School of Electrical and Computer Engineering, Cornell University, Ithaca, New York 14853*

Received March 7, 2006; revised April 28, 2006; accepted May 2, 2006; posted May 3, 2006 (Doc. ID 68743)

We demonstrate propagation losses of less than  $0.8 \text{ dB}/\mu\text{m}$  in a metal slot waveguide on silicon with a predicted confinement substantially below the optical wavelength ( $\sim 1.55 \mu\text{m}$ ). We also show compact and efficient coupling of the high-confinement metal slot waveguide with a standard silicon dielectric waveguide with a coupling efficiency of approximately 2.5 dB per facet. © 2006 Optical Society of America  
*OCIS codes:* 130.3120, 240.6680.

There is a growing research interest in optical circuits at the nanometer scale for future integration of optical, optoelectronic, and electronic devices on chips. For this goal, however, the typical dimensions of conventional dielectric waveguides are dictated by diffraction, therefore limiting dense on-chip integration. In contrast, plasmonic waveguides such as nanoparticle chains<sup>1</sup> and nanorods<sup>2</sup> guide light through the interaction of photon and electron oscillation around the metal surface and are potential candidates for nanoscale optical elements with sizes much smaller than the diffraction limit. The trade-off between the confinement level and the propagation loss, however, is a fundamental limitation of such waveguides. For example, for visible light, nanoparticle chains with confinements of approximately  $\lambda/5$  have been reported with propagation losses of  $30 \text{ dB}/\mu\text{m}$ .<sup>1</sup> Therefore structures offering both high confinement and relatively low loss are desired. Here we demonstrate a low-loss plasmonic waveguide with a predicted confinement substantially below the optical wavelength ( $\sim 1.55 \mu\text{m}$ ). We also demonstrate efficient integration of the plasmonic waveguide with dielectric silicon wire waveguides.

To overcome the traditional limitations of plasmonic waveguides,<sup>3</sup> we use an inverted metal slot waveguide with a dielectric core sandwiched between metal cladding.<sup>4</sup> As is general for surface plasmons, the electric field polarized perpendicular to the metal-dielectric interface is bound around the interfaces owing to the high dielectric discontinuity between metal and dielectric. When the two interfaces of the metal slot are brought closer together, the plasmonic waves around the two interfaces interact and result in a symmetrical mode where the light is almost completely confined in the dielectric slot, making extreme subwavelength confinement possible across the slot far beyond the diffraction limit. The effective index of the slot increases because of the coupled plasmonic waves.<sup>5</sup> Therefore for three-dimensional realistic structures the light is vertically confined by the index confinement mechanism. Confinement along this direction can also be significantly below the optical wavelength, since the effective index of the slot increases rapidly for a very narrow slot. Several two- or three-dimensional structures based on the idea of metal slots have been theoret-

ically analyzed.<sup>6,7</sup> Devices such as bends, splitters, Bragg reflectors, and nanocavities have been proposed.<sup>8,9</sup> Interferometers and ring resonators based on channel plasmon waveguides, which can be interpreted as metal slot waveguides with vertically tapering widths, were demonstrated very recently.<sup>10</sup> Experimental guiding through a slot in a thin metal film was reported,<sup>11</sup> and efficient coupling of a metal slot with a micrometer-size dielectric slab waveguide was recently predicted.<sup>12</sup> Here we show experimentally a low-loss metal-dielectric waveguide on a silicon substrate with predicted high confinement for infrared propagation. For what is the first time to our knowledge we measure the propagation losses of such waveguides and show experimentally high coupling efficiency between these waveguides and dielectric silicon waveguides using very compact tapers. The metal slot waveguide considered here is shown in Fig. 1(a). It consists of a silicon wire clad by gold, which in turn is embedded in silicon dioxide. Silicon is used as the slot because of its high refractive index and, more important, the convenient integration with silicon wire waveguides. A thin layer of silicon dioxide ( $\sim 80 \text{ nm}$ ) on top of the silicon isolates the field from the gold on the top. We calculate the eigenmodes and propagation loss of this structure by using a full-vectorial finite-difference mode solver.<sup>13</sup> For  $\lambda = 1550 \text{ nm}$ , a typical mode profile ( $|E_x|$ ) for a slot  $150 \text{ nm}$  wide and  $250 \text{ nm}$  thick is shown in Fig. 1(b), which shows high lateral confinement of the mode to a region of  $\sim 150 \text{ nm}$ . Since the lateral guiding mechanism is based on a coupled surface plasmon in-

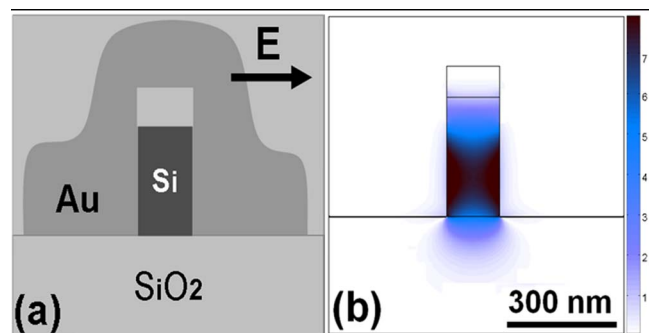


Fig. 1. (Color online) (a) Schematics and (b)  $|E_x|$ , mode profile of the metal slot waveguide with a  $150 \text{ nm}$  wide silicon core.

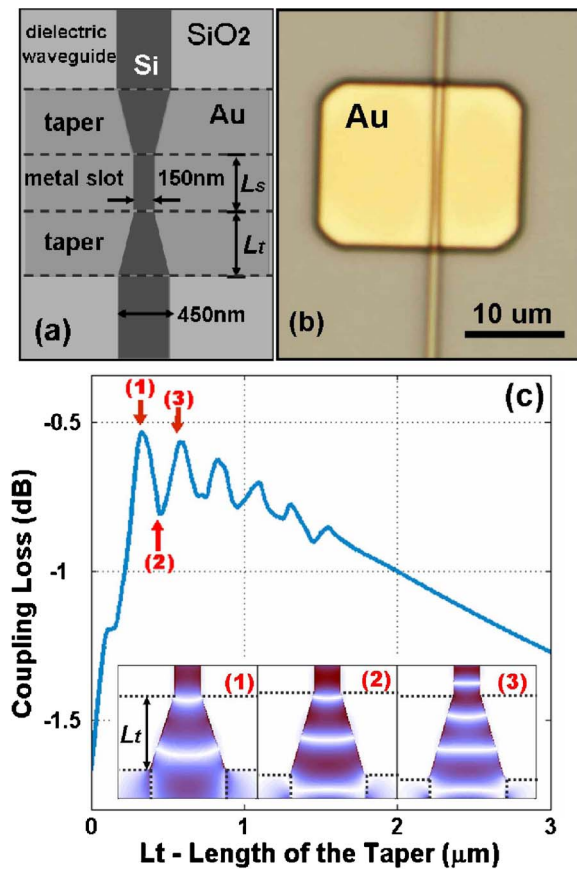


Fig. 2. (Color online) (a) Schematic and (b) microscope image of the metal slot integrated with a dielectric silicon wire waveguide. (c) FDTD simulation of the coupling loss versus the taper length for the 150 nm wide slot. Inset,  $E_x$  field distribution of the taper coupler for various taper lengths  $L_t$  as indicated by the arrows: (1) 325 nm, (2) 450 nm, and (3) 575 nm.

stead of an interference effect as is usual in pure dielectric waveguides, a similar mode profile remains even when the slot width shrinks to tens of nanometers. For a 150 nm slot, we calculate the loss due to absorption in the gold to be  $\sim 0.5$  dB/ $\mu\text{m}$ ; for a 50 nm slot, it increases to  $\sim 1.2$  dB/ $\mu\text{m}$ . This is at least 1 order of magnitude lower than what has been previously demonstrated with similar level of lateral confinement in nanoparticle chains.<sup>1</sup>

To integrate the slot waveguide with a 450 nm  $\times$  250 nm standard dielectric silicon wire waveguide, we use a compact linear taper to couple light in and out of the metal slot; see Fig. 2(a). There are three sources of loss in the taper: reflection at the metal-dielectric interface, propagation loss due to absorption in the metal, and reflection and radiation losses due to the tapering. Because of the high confinement of light in the input silicon wire waveguide, the interface reflection is less than 5%. The propagation loss through the taper could be estimated from the dependence of the loss coefficient on the slot width and monotonically increases with the taper length. However, for very sharp tapers, the tapering loss (due to reflection and radiation) dominates, and the overall coupling efficiency decreases. Therefore an optimal taper length exists due to the trade-off between these

two factors. We simulated the input coupling by using a three-dimensional finite-difference time-domain (FDTD) method for various taper lengths in the case of a 150 nm slot width [see Fig. 2(c)]. The  $E_x$  field distributions for three couplers of different lengths ( $L_t=325, 450, 575$  nm), are marked by the arrows in Fig. 2(c). One can see that for very short tapers ( $L_t < 300$  nm) the coupling efficiency drops rapidly. These are the taper dimensions for which the tapering losses dominate. For long tapers ( $L_t > 1.5$   $\mu\text{m}$ ), the loss due to the tapering is negligible, while the propagation loss due to absorption along the taper determines the coupling efficiency. Over this region we find a linear in the coupling efficiency. The most efficient coupling, with approximately 0.5 dB coupling loss, is obtained by using  $L_t \sim 325$  nm. In the range of maximum coupling efficiency one can see damping with the taper length. These oscillations are due to weak Fabry-Perot (FP) resonances inside the taper with a periodicity of  $\sim 225$  nm, consistent with the FP resonance period calculated by using  $L_{\text{FP}} = \lambda / 2n_{\text{eff}}$ , where  $n_{\text{eff}} \sim 3.4$  is the effective index of the medium estimated from the mode analysis. Note that in the case of zero taper length (the direct connection of the 450 nm wide silicon wire waveguide with the 150 nm slot) the coupling efficiency is 1.7 dB ( $\sim 68\%$  in power). This is because in the eigenmode of the 450 nm wide silicon wire waveguide the central 150 nm wide region has  $\sim 55\%$  of the total power, which results in the high coupling efficiency. For a much narrower slot, e.g., a 50 nm slot, the power confined in the central 50 nm wide region is only  $\sim 20\%$ , resulting in a coupling efficiency of 3.6 dB when no taper exists. With a similar compact linear taper, the coupling efficiency could be boosted to 0.7 dB. Note that, as is shown in Fig. 2(b), the field is enhanced in the narrow slot region after the taper because of a focusing effect of the plasmonic waves similar to those in metal tips<sup>14</sup> and grooves.<sup>15</sup>

We fabricated the metal slot waveguide on a silicon-on-insulator wafer with a silicon layer of 250 nm by electron-beam lithography patterning, followed by reactive ion etching. The exposed electron-beam resist acts as a thin layer of oxide for isolating. A photolithography step was then used with a bilayer photoresist structure to open the device window for metal evaporation. Note that, to allow for misalignment tolerances in the photolithography step, we used a longer than optimal taper ( $\sim 4$   $\mu\text{m}$ ), for which the coupling efficiency drops to about 2 dB estimated from the propagation loss. During evaporation the sample stage was slightly tilted and rotated to ensure close contact of the metal with the sidewalls of the silicon wire. After the liftoff process, the whole chip was covered with silicon dioxide through electron-beam evaporation. A microscope image of the device region is shown in Fig. 2(b).

Experimentally, we coupled polarized laser light at  $\lambda = 1550$  nm from a tapered lens fiber to the silicon wire waveguides terminated with nanotapers<sup>16</sup> and measured the transmitted power by using an infra-

red detector. Figure 3(a) shows a typical plot of the normalized power versus the length of the metal slot waveguide for a slot width of 150 nm. The transmitted power is normalized to a reference dielectric waveguide with no metal slot; therefore the normalization gives the loss due to the devices. From the linear fit, we find the propagation and the coupling loss for the 150 nm wide slot to be about  $0.8 \text{ dB}/\mu\text{m}$  and  $\sim 2.5 \text{ dB}$  per facet, respectively, both values close to the theoretical predictions. In Fig. 3(b) we show the measured propagation loss for a different slot width compared with the simulation results, demonstrating a relatively good agreement between the two. The 150 nm slot is the narrowest device we fabricated. For an even narrower slot, e.g., 50 nm, we expect the loss to be  $2\text{--}3 \text{ dB}/\mu\text{m}$ . This loss level is at least 1 order of magnitude lower than what has been previously demonstrated with comparable degrees of lateral confinement.

In conclusion, we demonstrate a metal slot waveguide with deep subwavelength confinement and propagation loss that is 1 order of magnitude lower than previously demonstrated with comparable degrees of lateral confinement. With a compact taper about  $4 \mu\text{m}$  long, we also demonstrate integration of the metal slot and silicon wire with a high coupling

efficiency of about  $2.5 \text{ dB}$  per facet. Using an optimal taper length of less than  $0.5 \mu\text{m}$ , the coupling loss is expected to be reduced to about  $0.5 \text{ dB}$ . The realization of deep subwavelength confinement and efficient coupling with standard dielectric silicon waveguides has attractive applications in nanoscale circuits and on-chip integration of optical, optoelectronic, and electronic devices.

The authors acknowledge Christina Manolatu for her assistance in the simulations. This work was supported by the Science and Technology Centers program of the National Science Foundation under agreement DMR-0120967, the Semiconductor Research Corporation under grant 2005-RJ-1296, the Cornell Center for Nanoscale Systems, the Cornell Center for Material Research, and the National Science Foundation's CAREER grant 0446571. The authors also thank Gernot Pomrenke from the Air Force Office of Scientific Research for supporting the work under grants F49620-03-1-0424 and FA9550-05-C-0102. This work was performed in part at the Cornell Nanoscale Science and Technology Facility, a member of the National Nanotechnology Infrastructure Network, which is supported by the National Science Foundation under grant ECS-9731293, its users, Cornell University, and industrial affiliates. M. Lipson's e-mail address is lipson@ece.cornell.edu; L. Chen's e-mail address is lc286@cornell.edu.

## References

1. S. A. Maier, P. G. Kik, H. A. Atwater, S. Meltzer, E. Harel, B. E. Koel, and A. A. G. Requicha, *Nat. Mater.* **2**, 229–232 (2003).
2. J. Takahara, S. Yamaguchi, H. Taki, A. Morimoto, and T. Kobayashi, *Opt. Lett.* **22**, 475 (1997).
3. J. C. Weeber, Y. Lacroute, and A. Dereux, *Phys. Rev. B* **68**, 115401 (2003).
4. R. Zia, M. D. Selker, P. B. Catrysse, and M. L. Brongersma, *J. Opt. Soc. Am. A* **21**, 2442 (2004).
5. K. Tanaka and M. Tanaka, *Appl. Phys. Lett.* **82**, 1158 (2005).
6. L. Liu, Z. Han, and S. He, *Opt. Express* **13**, 6645 (2005).
7. G. Veronis and S. Fan, *Opt. Lett.* **30**, 3359 (2005).
8. G. Veronis and S. Fan, *Appl. Phys. Lett.* **87**, 131102 (2005).
9. B. Wang and G. Wang, *Appl. Phys. Lett.* **87**, 013107 (2005).
10. S. I. Bozhevolnyi, V. S. Volkov, E. Devaux, J. Laluet, and T. W. Ebbesen, *Nature* **440**, 508 (2006).
11. D. F. P. Pile, T. Ogawa, D. K. Gramotnev, Y. Matsuzaki, K. C. Vernon, K. Yamaguchi, T. Okamoto, M. Haraguchi, and M. Fukui, *Appl. Phys. Lett.* **87**, 261114 (2005).
12. P. Ginzburg, D. Arbel, and M. Orenstein, in *Conference on Lasers and Electro-optics* (Optical Society of America, 2005), paper CWN5.
13. C. L. Xu, W. P. Huang, M. S. Stern, and S. K. Chaudhuri, *IEEE Proc.: Optoelectron.* **141**, 281 (1994).
14. M. I. Stockman, *Phys. Rev. Lett.* **93**, 137404 (2004).
15. D. K. Gramotnev, *J. Appl. Phys.* **98**, 104302 (2005).
16. V. R. Almeida, R. R. Panepucci, and M. Lipson, *Opt. Lett.* **28**, 1302 (2003).

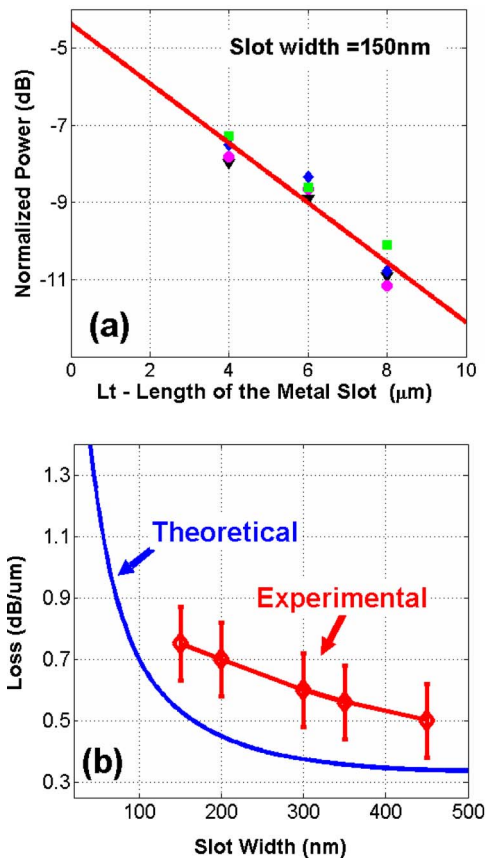


Fig. 3. (Color online) (a) Normalized transmitted power versus length of the metal slot waveguide for a slot width of 150 nm. (b) Theoretical and experimental propagation losses for several slot waveguides with different slot widths.